Verification of universal relations in a strongly interacting Fermi gas

J. T. Stewart, J. P. Gaebler,* T. E. Drake, and D. S. Jin†

JILA, Quantum Physics Division, National Institute of
Standards and Technology and Department of Physics,
University of Colorado, Boulder, CO 80309-0440, USA

(Dated: October 31, 2018)

Abstract

Many-body fermion systems are important in many branches of physics, including condensed matter, nuclear, and now cold atom physics. In many cases, the interactions between fermions can be approximated by a contact interaction. A recent theoretical advance in the study of these systems is the derivation of a number of exact universal relations that are predicted to be valid for all interaction strengths, temperatures, and spin compositions [1–6]. These equations, referred to as the Tan relations, relate a microscopic quantity, namely, the amplitude of the high-momentum tail of the fermion momentum distribution, to the thermodynamics of the many-body system. In this work, we provide experimental verification of the Tan relations in a strongly interacting gas of fermionic atoms. Specifically, we measure the fermion momentum distribution using two different techniques, as well as the rf excitation spectrum and determine the effect of interactions on these microscopic probes. We then measure the potential energy and release energy of the trapped gas and test the predicted universal relations.

In 2008, Shina Tan derived a number of universal relations for an interacting Fermi gas with short-range, or contact, interactions [1–3]. These relations are very powerful because they connect microscopic quantities, such as the momentum distribution of the fermions, to macroscopic quantities, such as the total energy of the system. Furthermore, the relations are universal in that they do not depend on the details of the interparticle potential that gives rise to the interaction, nor do they depend on the state of the system, which could be an exotic Fermi superfluid, a normal Fermi liquid, or even a simple two-body state such as a diatomic molecule composed of two fermionic atoms. At the heart of the universal relations is a single quantity, which Tan termed the contact. The contact is defined as the amplitude of the high-k tail of the momentum distribution $n(k)$, which was previously predicted to scale as $1/k^4$ for an interacting Fermi gas [7]. Remarkably, it can be shown that the contact encapsulates all of the many-body physics [6]. Therefore, it is predicted that by measuring this tail of the momentum distribution and then applying universal relations, one could determine many other properties of the system. Two recent papers report the contact for a strongly interacting Fermi gas, extracted from photoassociation measurements [5, 8] and inelastic Bragg spectroscopy [9] and compare the results with theoretical predictions for the BCS-BEC crossover. Here, we present a series of measurements that not only measure the contact in the BCS-BEC crossover with two different techniques, but moreover test the Tan relations experimentally by comparing measurements of both microscopic and macroscopic quantities in the same system. Our results directly verify the universal relations by exploiting the fact that while the value of the contact depends on the many-body state and on parameters such as temperature, number density, and interaction strength, the universal relations do not.

Our measurements are done in an ultra cold gas of fermionic ^{40}K atoms confined in a harmonic trapping potential. We cool the gas to quantum degeneracy in a far-detuned optical dipole trap as described in previous work [10]. The trap is axially symmetric and parameterized by a radial trap frequency, which varies for these data from $\omega_r = 2\pi \cdot 230$ to $2\pi \cdot 260$ Hz and an axial trap frequency, which varies from $\omega_z = 2\pi \cdot 17$ to $2\pi \cdot 21$ Hz. We obtain a 50/50 mixture of atoms in two spin states, namely the $|f, m_f\rangle = |9/2, -9/2\rangle$ and $|9/2, -7/2\rangle$ states, where f is the total atomic spin and m_f is the projection along the magnetic-field axis. Our final stage of evaporation occurs at a magnetic field of 203.5 G, where the s-wave scattering length, a, that characterizes the interactions between atoms in the $|9/2, -9/2\rangle$ and $|9/2, -7/2\rangle$ states is approximately 800 a_0, where a_0 is the Bohr radius.

At the end of the evaporation, we have 10^5 atoms per spin state at a normalized temperature $\frac{T}{T_F} = 0.11 \pm 0.02$ where the Fermi temperature corresponds to the Fermi Energy, $E_F = k_b T_F = \hbar\omega(6N)^{1/3}$ where N is the total atom number in one spin state and $\omega = (\omega_r^2 \omega_z)^{1/3}$ and k_b is the the Boltzmann constant. After the evaporation we increase the interaction strength adiabatically with a slow magnetic-field ramp to a Fano-Feshbach scattering resonance.

The momentum distribution of the fermions, $n(k)$, is predicted to scale as $1/k^4$ at high k, with the contact being the coefficient of this high momentum tail. Following Tan [2], we define the integrated contact per particle for the trapped gas, which we will refer to simply as the contact, using

$$C = \lim_{k \to \infty} k^4 n(k). \tag{1}$$

Here, k is the wave number in units of the Fermi wave number, $k_F = \frac{2mE_F}{\hbar}$, and $n(k)$ for a 50/50 spin mixture is normalized such that $\int_0^\infty \frac{n(k)}{(2\pi)^3} d^3k = 0.5$. Note that the contact is expected to be the same for both spin states in the interacting Fermi gas, even in the case of an imbalanced spin mixture. Theoretically, the contact is defined in the limit of $1 << k << 1/(k_F r_0)$, where r_0 is the range of the interatomic potential. Using a typical value of $k_F = \frac{1}{2200} a_0^{-1}$ for our trapped ^{40}K gas and the van der Waals length, $r_0 = 60a_0$, we find $1/(k_F r_0) = 37$.

We directly measure $n(k)$ using ballistic expansion of the trapped gas, where we turn off the interactions for the expansion. We accomplish this by rapidly sweeping the magnetic field to 209.2 G where a vanishes, and then immediately turning off the external trapping potential [11]. We let the gas expand for 6 ms before taking an absorption image of the cloud. The probe light for the imaging propagates along the axial direction of the trap and thus we measure the radial momentum distribution. Assuming the momentum distribution is spherically symmetric, we obtain the full momentum distribution with an inverse Abel transform.

Fig. 1a shows an example $n(k)$ for a strongly interacting gas measured with this technique. For this data, the dimensionless interactions strength $(k_F a)^{-1}$, is -0.08 ± 0.10. Empirically, we find that the measured $n(k)$ exhibits a $1/k^4$ tail and we extract the contact C from the average value of $k^4 n(k)$ for $k > k_C$ where we use $k_C = 1.85$ for $(k_F a)^{-1} > -0.5$, and $k_C = 1.55$ for $(k_F a)^{-1} < -0.5$. One issue is whether or not the interactions are switched off sufficiently quickly to accurately measure the high-k part of the $n(k)$. The data in
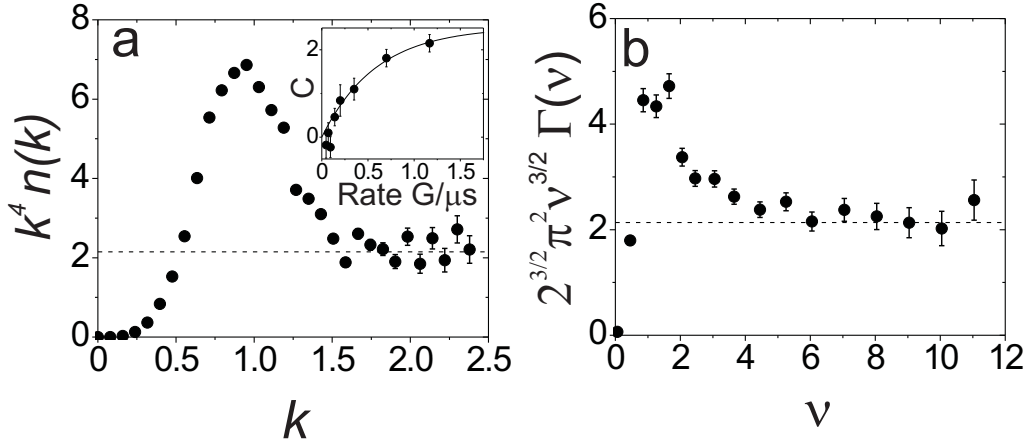
3

FIG. 1: **Extracting the contact from the momentum distribution and rf lineshape.** (a) Measured momentum distribution for a Fermi gas at $\frac{1}{k_F a} = -0.08 \pm 0.10$. Here, the wave number k is given in units of k_F, and we plot the normalized $n(k)$ multiplied by k^4. The dashed line corresponds to $C = 2.15 \pm 0.2$, which is obtained by averaging $k^4 n(k)$ for $k > 1.85$. (Inset) The measured value for C depends on the rate of the magnetic-field ramp that turns off the interactions before time-of-flight expansion. (b) RF lineshape measured for a Fermi gas at $\frac{1}{k_F a} = -0.03 \pm 0.10$. Here, ν is the rf detuning from the single-particle Zeeman resonance, given in units of E_F/h. We plot the normalized rf lineshape multiplied by $2^{3/2}\pi^2\nu^{3/2}$, which is predicted to asymptote to C for large ν. Here, we obtain $C = 2.13 \pm 0.2$ (dashed line) from an average of the data for $\nu > 5$.

Fig. 1a were taken using a magnetic-field sweep rate of approximately $1.4\frac{G}{\mu s}$ to turn off the interactions for the expansion. In the inset to Fig. 1a, we show the dependence of the measured C on the magnetic-field sweep rate. Using an empirical exponential fit (line in Fig. 1a inset), we estimate that at our typical sweep rate of approximately $1.4\frac{G}{\mu s}$ our measured C is systematically low by about 10%. We have therefore scaled the contact measured with this method by 1.1.

The contact is also manifest in rf spectroscopy, where one applies a pulsed rf field and counts the number of atoms that are transferred from one of the two original spin states into a third, previously unoccupied, spin state [12]. We transfer atoms from the $|9/2, -7/2\rangle$ state to the $|9/2, -5/2\rangle$ state. It is predicted that the number of atoms transferred as a function of the rf frequency, ν, scales as $\nu^{-3/2}$ for large ν, and that the amplitude of this high frequency tail is $\frac{C}{2^{3/2}\pi^2}$ [13–15]. Here, $\nu = 0$ is the single-particle spin-flip resonance,

and ν is given in units of E_F/h. This prediction requires that atoms transferred to the third spin-state have only weak interactions with the other atoms, so that "final state effects" are negligible [15–22], as is the case for ^{40}K atoms. In Fig. 1b, we plot a measured rf spectrum multiplied by $2^{3/2}\pi^2\nu^{3/2}$. The rf spectrum, $\Gamma(\nu)$, is normalized so that the integral over the rf lineshape equals 0.5. Empirically, we observe the predicted $1/\nu^{3/2}$ behavior for $\nu > \nu_C$. To obtain the contact we average $2^{3/2}\pi^2\nu^{3/2}\Gamma(\nu)$ for $\nu > \nu_C$ where $\nu_C = 5$ for $(k_F a)^{-1} > -0.5$, and $\nu_C = 3$ for $(k_F a)^{-1} < -0.5$.

The connection between the tail of the rf spectrum and the high-k tail of the momentum distribution can be seen in the Fermi spectral function, which can be probed using photoemission spectroscopy for ultra cold atoms [10]. Recent photoemission spectroscopy results on a strongly interacting Fermi gas [23] revealed a weak, negatively dispersing feature at high k that persists to temperatures well above T_F. This feature was attributed to the effect of interactions, or the contact, consistent with a recent prediction that the $1/k^4$ tail in $n(k)$ should correspond to a high-k part of the spectral function that disperses as $-k^2$ [24]. Atom photoemission spectroscopy, which is based upon momentum-resolved rf spectroscopy, also provides a method for measuring $n(k)$. By integrating over the energy axis, or equivalently, summing data taken for different rf frequencies, we obtain $n(k)$. This alternative method for measuring $n(k)$ yields results similar to the ballistic expansion technique, but avoids the issue of magnetic-field ramp rates.

In Fig. 2 we show the measured contact for different values of the dimensionless interaction strength, $1/k_F a$. Here, the contact is extracted using the three different techniques described above to probe two distinct microscopic quantities, namely the momentum distribution and the rf lineshape. We find that the amplitude of the $1/k^4$ tail of $n(k)$ and the coefficient of the $1/\nu^{3/2}$ tail of the rf spectra yield consistent values for C. The solid line is a prediction for the contact that was reported in Fig. 1 of Ref. [5]. This prediction consists of the BCS limit, interpolation of Monte Carlo data near unitarity, and the BEC limit for a trapped gas at zero temperature and uses a local density approximation.

Remarkably, the Tan relations predict that the contact, as revealed in probes of the microscopic behavior of the gas, is directly connected to the thermodynamics of the gas. To test the Tan relations, we measure the potential energy and release energy of the cloud. The total energy of the trapped gas divided by the number of particles, E, is the sum of three contributions, the kinetic energy T, the external potential energy V, and the interaction
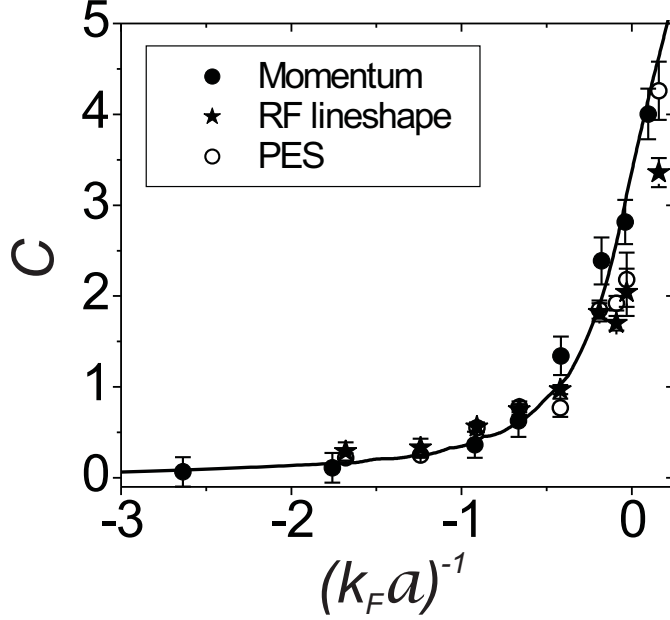
5

FIG. 2: **The contact.** We measure the contact, C, as a function of $(k_F a)^{-1}$ using three different methods. Filled circles correspond to direct measurements of the fermion momentum distribution $n(k)$ using a fast magnetic-field sweep to project the many-body state onto a non-interacting state. The momentum distribution can then be measured in ballistic expansion. Open circles correspond to $n(k)$ obtained using atom photoemission spectroscopy measurements. Stars correspond to the contact obtained from rf spectroscopy. The values obtained with these different methods show good agreement. The contact is nearly zero for a weakly interacting Fermi gas with attractive interactions (left hand side of plot) and then increases as the interaction strength increases to the unitarity regime where $(k_F a)^{-1} = 0$. The line is a theory curve obtained from Ref. [5]

.

energy I. Because the momentum distribution has a $1/k^4$ tail, the kinetic energy obtained by integrating over the momentum distribution diverges. However, the release energy $T + I$, which can be measured in the usual time-of-flight expansion without turning off the interactions, is not divergent.

We measure V by imaging the spatial distribution of the atom cloud, similar to measurements that were performed in Ref. [25]. We allow the cloud to expand for 1.6 ms to lower the optical density and then image along one of the radial directions in order to see the density distribution in the axial direction. Because the expansion time is short compared

to the axial trap period (40 times shorter) the density distribution in the axial direction reflects the in-trap axial density distribution. The potential energy per particle, in units of E_F, is then $V = \frac{3}{NE_F} \frac{1}{2} m\omega_z^2 \langle z^2 \rangle$, where $\langle z^2 \rangle$ is the mean squared width of the cloud in the axial direction and we have assumed that the total potential energy is distributed equally over the three axes.

To measure the release energy $T + I$ we turn off the trap suddenly and let the cloud expand for $t = 16$ ms (with interactions) before imaging along one of the radial directions; this is similar to measurements reported in Ref. [26]. The total release energy is the sum of the release energy in the two radial directions and the release energy in the axial direction. For the radial direction, the release energy per particle, in units of E_F, is simply $T_r + I_r = \frac{2}{NE_F} \frac{1}{2} m \frac{\langle y^2 \rangle}{t^2}$ where t is the expansion time and $\langle y^2 \rangle$ is the mean squared width of the expanded cloud in the radial direction. For the axial direction, the expansion is slower and the expanded cloud may not be much larger than the in-trap density distribution. This is especially true near the Feshbach resonance where the cloud expands hydrodynamically [27]. Accounting for this, the axial release energy is $T_z + I_z = \frac{1}{NE_F} \frac{1}{2} m \frac{\langle z^2 \rangle - z_0^2}{t^2}$, where z_0^2 is mean squared axial width of the in-trap density distribution. We extract the mean squared cloud widths from surface fits to the images, where we fit to a finite temperature Fermi Dirac distribution while minimizing the difference in energy between the raw data and the fit. Rather than being theoretically motivated, we simply find empirically that this functional form fits well to our images. To eliminate systematic error due to uncertainty in the trap frequencies and imaging magnification, we measure the release energy and potential energy of a very weakly interacting Fermi gas at $\frac{T}{T_F} = 0.11$, where $T + I$ and V for an ideal Fermi gas is $0.40E_F$. We then use the ratio of $0.40E_F$ to our measured values as a multiplicative correction factor that we apply to all of the data. This correction is within 5% of unity. For the point with $\frac{1}{k_F a} > 0$ we take into account the binding energy of the molecules in our tabulation of the release energy $T + I$ by adding $-1/(k_F a)^2$. We show our data for the V and $T + I$ versus $(k_F a)^{-1}$ in the inset of Fig. 3.

We can now test the predicted universal relations connecting the $1/k^4$ tail of the momentum distribution with the thermodynamics of the trapped Fermi gas. We first consider the adiabatic sweep theorem [1],

$$2\pi \frac{dE}{d(-1/(k_F a))} = C, \qquad (2)$$

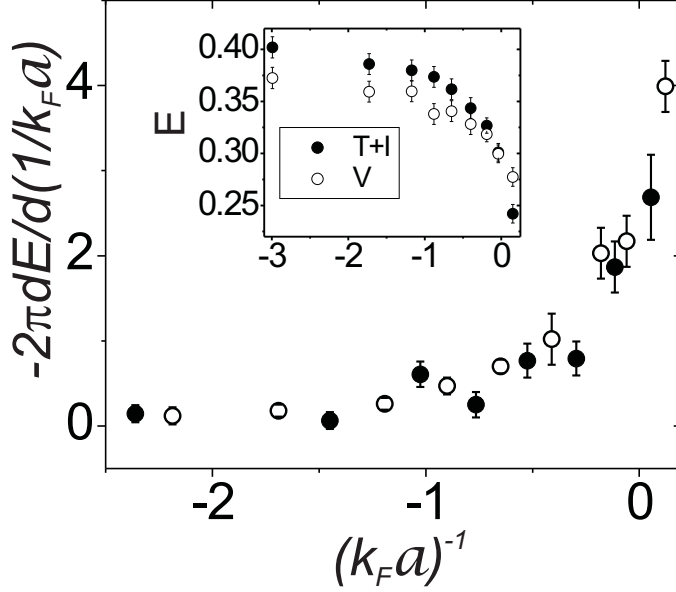which relates the contact C to the change in the total energy of the system when the

FIG. 3: **Testing the adiabatic sweep theorem.** (Inset) The measured potential energy, V, and release energy, $T + I$, per particle in units of E_F is shown as a function of $1/k_F a$. (Main) Taking a discrete derivative of the data shown in the inset, we find that $2\pi \frac{dE}{d(-1/(k_F a))}$ (●) agrees well with the contact C measured from the high-k tail momentum distribution (○).

interaction strength is changed adiabatically. To obtain the energy per particle, E, we sum the values for $T + I$ and V shown in the inset of Fig. 3. To test the adiabatic sweep theorem, we find the derivative, $\frac{dE}{d(-1/(k_F a))}$, simply by calculating the slope for pairs of neighboring points in the inset to Fig. 3. In the main part of Fig. 4, we compare this point-by-point derivative, multiplied by 2π, to C obtained from the average values of the data shown in Fig. 2(○). Comparing these measurements of the left and right sides of Eqn. 2, we find good agreement and thus verify the adiabatic sweep theorem for our strongly interacting Fermi gas.

A second universal relation that we can directly test is the generalized virial theorem [2],

$$E - 2V = T + I - V = -\frac{C}{4\pi k_F a}, \tag{3}$$

which relates the difference between the release energy and the potential energy to the contact. Eqn. 3 is predicted to be valid for all values of the interaction strength $(k_F a)^{-1}$. This generalized virial theorem reduces to $E - 2V = 0$ for the ideal gas, where $I = 0$, as well
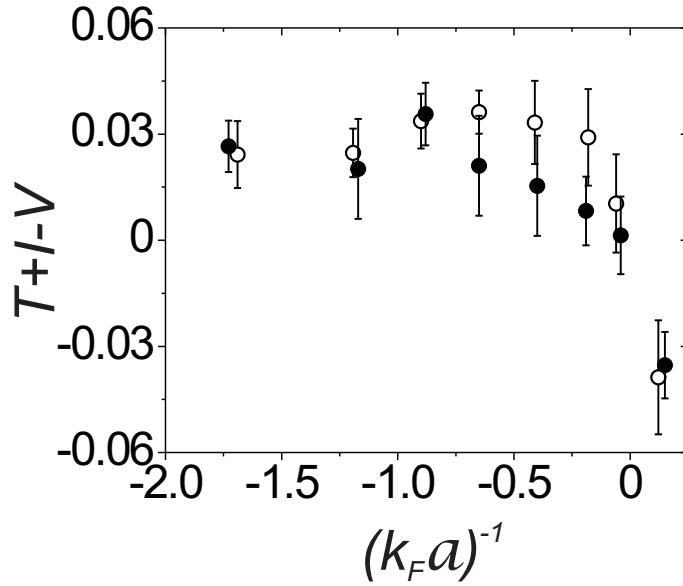
8

FIG. 4: **Testing the generalized virial theorem.** The difference between the measured release energy and potential energy per particle $T+I-V$ is shown as open circles. This corresponds to the left hand side of Eq. 3. Filled circles show the right hand side of Eq. 3 obtained from the average values of the contact shown in Fig. 2. The two quantities are equal to within the measurement uncertainty, which is on order of $0.01E_F$.

as for the unitarity gas, where $(k_F a)^{-1} = 0$. This result for the unitarity gas was previously verified in Ref. [28]. Here, we test Eqn. 3 for a range of interaction strengths. In Fig. 4 we plot the measured difference $T + I - V$ versus $(k_F a)^{-1}$ along with $\frac{C}{4\pi k_F a}$, where we use our direct measurements of C. We find that these independent measurements of the left and the right sides of Eqn. 3 agree to within our error, which is roughly 1% of the Fermi energy. It is interesting to note that the measured energy difference $T + I - V$ is small (in units of E_F), so that even a Fermi gas with a strongly attractive contact interaction nearly obeys the non-interacting virial equation.

In conclusion, we have measured the integrated contact for a strongly interacting Fermi gas and demonstrated the connection between the $1/k^4$ tail of the momentum distribution and the high frequency tail of rf spectra. Combining a measurement of C vs $(k_F a)^{-1}$ with measurements of the potential energy and the release energy of the trapped gas, we verify two universal relationships [2, 3], namely the adiabatic sweep theorem and the generalized

9

virial theorem. These universal relations, which have now been experimentally confirmed, represent a significant advance in the understanding of many-body quantum systems with strong short-range interactions. Furthermore, these connections between microscopic and macroscopic quantities could be exploited to develop novel experimental probes of the many-body physics of strongly interacting quantum gases.

---

* Electronic address: gaeblerj@jila.colorado.edu

† URL: `http://jilawww.colorado.edu/~jin/`

[1] S. Tan, Ann. Phys. **323**, 2971 (2008).

[2] S. Tan, Ann. Phys. **323**, 2987 (2008).

[3] S. Tan, Ann. Phys. **323**, 2952 (2008).

[4] E. Braaten, and L. Platter, Phys. Rev. Lett. **100**, 205301 (2008).

[5] F. Werner, L. Tarruel, and Y. Castin, Eur. Phys. J. B **68**, 401 (2009).

[6] S. Zhang and A. J. Leggett, Phys. Rev. A **79**, 023601 (2009).

[7] L. Viverit, S. Giorgini, L. P. Pitaevskii, and S. Stringari, Phys. Rev. A **69**, 013607 (2004).

[8] G. B. Partridge *et al.*, Phys. Rev. Lett. **95**, 020404 (2005).

[9] H. Hu *et al.*, arXiv:1001.3200 (unpublished).

[10] J. T. Stewart, J. P. Gaebler, and D. S. Jin, Nature **454**, 744 (2008).

[11] C. A. Regal *et al.*, Phys. Rev. Lett. **95**, 250404 (2005).

[12] C. A. Regal, C. Ticknor, J. L. Bohn, and D. S. Jin, Nature **424**, 47 (2003).

[13] P. Pieri, A. Perali, and G. C. Strinati, Nat. Phys. **5**, 736 (2009), arXiv:0811.0770.

[14] W. Schneider, V. B. Shenoy, and M. Randeria, arXiv:0903.3006v1 (unpublished).

[15] E. Braaten, D. Kang, and L. Platter, arXiv:1001.4518v1 (unpublished).

[16] C. Chin and P. S. Julienne, Phys. Rev. A **71**, 012713 (2005).

[17] Z. Yu and G. Baym, Phys. Rev. A **73**, 063601 (2006).

[18] M. Punk and W. Zwerger, Phys. Rev. Lett. **99**, 170404 (2007).

[19] S. Basu and E. J. Mueller, arXiv:0712.1007v1 (unpublished).

[20] A. Perali, P. Pieri, and G. C. Strinati, Phys. Rev. Lett. **100**, 010402 (2008).

[21] M. Veillette *et al.*, Phys. Rev. A **78**, 033614 (2008), arXiv:0803.2517v1.

[22] Y. He, C. C. Chien, Q. Chen, and K. Levin, Phys. Rev. A **77**, 011602(R) (2008).

[23] J. P. Gaebler *et al.*, Observation of pseudogap phase in a strongly interacting Fermi gas, 2010, to be submitted for publication.

[24] W. Schneider and M. Randeria, arXiv:0910.2693 (unpublished).

[25] J. T. Stewart, J. P. Gaebler, C. A. Regal, and D. S. Jin, Phys. Rev. Lett. **97**, 220406 (2006).

[26] T. Bourdel *et al.*, Phys. Rev. Lett. **91**, 020402 (2003).

[27] K. M. O'Hara *et al.*, Science **298**, 2179 (2002).

[28] J. E. Thomas, J. Kinast, and A. Turlapov, Phys. Rev. Lett. **95**, 120402 (2005).